

A complete bifurcation analysis of planar conewise affine systems^{*}

J. J. Benjamin Biemond^{*} Nathan van de Wouw^{*}
Henk Nijmeijer^{*}

^{*} *Department of Mechanical Engineering, Eindhoven University of Technology, P.O. Box 513, 5600 MB Eindhoven, The Netherlands, email: j.j.b.biemond@tue.nl*

Abstract: In this paper we present a procedure to find all limit sets near bifurcating equilibria in continuous, piecewise affine systems defined on a conic partition of the plane. To guarantee completeness of the obtained limit sets, new conditions for the existence or absence of closed orbits are combined with the study of return maps. With these results a complete bifurcation analysis of a class of planar conewise affine systems is presented.

Keywords: Nonlinear systems, bifurcations, limit cycles, stability analysis, hybrid systems, piecewise linear systems.

1. INTRODUCTION

In this paper, local bifurcations are studied of continuous, piecewise smooth dynamical systems. These systems occur in mechanical, electrical, biological or economical systems, see e.g. Leine and Nijmeijer (2004); Liberzon (2003); Coombes (2008); Oberle and Rosendahl (2006). Such systems can exhibit so-called discontinuity-induced bifurcations, see Leine and Nijmeijer (2004); di Bernardo et al. (2008b). In this paper, we study discontinuity-induced bifurcations of equilibria in planar systems and we present a procedure to find all limit sets, which are created or destroyed by the bifurcation of an equilibrium.

The state space of piecewise smooth systems can be partitioned in a number of domains where the dynamics is smooth, and their boundaries, where the dynamics is nonsmooth. Discontinuity-induced bifurcations are topological changes in behaviour when system parameters are varied around the values where a limit set collides with such a boundary. Although the effect of such bifurcations is observed both in simulations and experiments, Leine and Nijmeijer (2004); di Bernardo et al. (2008b), no complete theory is available to describe these bifurcations.

In planar systems, limit sets can be equilibria, closed orbits (including limit cycles), homoclinic or heteroclinic orbits. Discontinuity-induced bifurcations of closed orbits and homoclinic or heteroclinic orbits can be studied by taking a Poincaré section transversal to these orbits and analysing the resulting return map. In this manner, bifurcations of limit cycles in piecewise smooth systems are rather well understood, cf. Nordmark (1991); di Bernardo et al. (2008b).

Bifurcations of equilibria are studied among others in Leine (2006); di Bernardo et al. (2008a,b), where at the bifurcation point the equilibrium is positioned on a single, smooth boundary. However, no theoretical result is available when this equilibrium is positioned on multiple boundaries or when the boundary is locally nonsmooth. Existence of such bifurcations was recognized in numerical

simulations of exemplary systems in Leine et al. (2000); Leine (2006). In this paper, we study continuous systems, where the dynamics is affine with respect to the system parameter in each smooth domain, that is a cone. These systems are called conewise affine systems.

The main contribution of this paper is a procedure for planar, continuous, conewise affine systems to find all limit sets that can be created or destroyed during the bifurcation of an equilibrium, when the system dynamics is dependent on the bifurcation parameter in an affine term. To exclude closed orbits in certain regions of state space, Bendixson's Theorem and index theory are used. To obtain all closed orbits in the remaining part of the state space, return maps are derived, whose Poincaré sections are chosen at locations, determined by the investigation of specific trajectories. Fixed points of these return maps determine the existence and stability of limit cycles or closed orbits.

In addition, we derive general conditions for the existence of a halfline, that can not be traversed by closed orbits. Using these conditions, one can guarantee that all limit sets are found with the given procedure. According to index theory, closed orbits should encircle at least one equilibrium point. Derivation of all possible return maps for the trajectories that cross a line between the equilibria and the halfline will yield all existing closed orbits. The domain of these return maps is bounded, such that fixed points can be detected with numerical methods.

Although the Poincaré-Bendixson theorem can be used to give sufficient conditions for the existence of limit cycles, c.f. Hartman (1964), we derive conditions that are necessary and sufficient using a different approach.

This paper is organized as follows. In Section 2 some preliminary results are given. Subsequently, in Section 3 the stability of an equilibrium at the bifurcation point is investigated. In Section 4 the main theoretical results of this paper are presented, together with the procedure to find all limit sets near the bifurcation point. This procedure is illustrated with an example in Section 5. Finally, conclusions are formulated in Section 6.

^{*} Supported by the European Network of Excellence HYCON (FP6-IST-511368) and by the Netherlands Organisation for Scientific Research (NWO).

2. PRELIMINARIES

We consider a conewise affine system, that is described by:

$$\dot{\mathbf{x}} = \mathbf{f}(\mathbf{x}, \mu) := A_i \mathbf{x} + \mu \mathbf{b}, \quad \mathbf{x} \in \mathcal{S}_i, \quad (1)$$

where all regions \mathcal{S}_i , $i = 1, 2, \dots, m$, are open cones coinciding at the origin. The matrices A_i are such, that the function $\mathbf{f}(\mathbf{x}, \mu)$ is continuous. The vector \mathbf{b} can always be chosen to satisfy $\|\mathbf{b}\| = 1$. Here, $\|\cdot\|$ denotes the Euclidian norm of a vector. The dynamics of this system is studied for varying bifurcation parameter μ . The indices i of the regions \mathcal{S}_i , $i = 1, \dots, m$, are chosen such, that the set $\{\mathcal{S}_1, \dots, \mathcal{S}_m\}$ is ordered in counter clockwise direction. Let Σ_{ij} be the boundary between the cones \mathcal{S}_i and \mathcal{S}_j and let $\{\mathbf{t}_{12} \dots \mathbf{t}_{m-1,m}, \mathbf{t}_{m1}\}$ be the set of distinct unit vectors in \mathbb{R}^2 parallel to the boundaries $\Sigma_{12} \dots \Sigma_{m-1,m}, \Sigma_{m1}$. Define $\mathbf{t}_{01} := \mathbf{t}_{m1}$ and $\Sigma_{01} := \Sigma_{m1}$, such that each \mathcal{S}_i is bounded by $\Sigma_{i-1,i} = \{\mathbf{x} \in \mathbb{R}^2 | \mathbf{x} = c \mathbf{t}_{i-1,i}, c \in [0, \infty)\}$ and $\Sigma_{i,i+1} = \{\mathbf{x} \in \mathbb{R}^2 | \mathbf{x} = c \mathbf{t}_{i,i+1}, c \in [0, \infty)\}$. With parameter $\mu = 0$, the system is called conewise linear.

In this paper, the following definition of a cone is used, that is an adapted version of the definition given in Camlibel et al. (2008).

Definition 1. Consider a region $\mathcal{S} \subset \mathbb{R}^n$. If $\mathbf{x} \in \mathcal{S}$ implies $c\mathbf{x} \in \mathcal{S}, \forall c \in (0, \infty)$ and $\mathcal{S} \setminus \{\mathbf{0}\}$ is connected and convex, then \mathcal{S} is a cone.

In this paper, $\bar{\mathcal{S}}$ denotes the closure of the open set \mathcal{S} .

Definition 2. Let $\dot{\mathbf{x}} = A_i \mathbf{x} + \mu \mathbf{b}$ be the dynamics on an open cone $\mathcal{S}_i \subset \mathbb{R}^2$, $i = 1, \dots, m$. An eigenvector of A_i is visible if it lies in $\bar{\mathcal{S}}_i$.

System (1) contains a visible eigenvector when a cone $\bar{\mathcal{S}}_i$ contains a visible eigenvector of the corresponding matrix A_i .

Based on the index theory presented in Coddington and Levinson (1955), we can formulate the following theorem.

Theorem 1. Inside a closed orbit C of the planar dynamical system $\dot{\mathbf{x}} = \mathbf{f}(\mathbf{x})$, where $\mathbf{f} : E \rightarrow \mathbb{R}^2$ is a Lipschitz continuous function, at least one equilibrium point exists. If all equilibria inside C are hyperbolic nodes, saddles, or foci, then there must be an odd number $2n+1$ of equilibria, where n is an integer, such that n equilibria are saddles and $n+1$ equilibria are nodes or foci.

The proofs of this and subsequent results can be found in Biemond et al. (2009), and are omitted here for the sake of brevity. Moreover, the following extension of Bendixson's Theorem is used.

Theorem 2. (Branicky (1998)). Suppose E is a simply connected domain in \mathbb{R}^2 and $\mathbf{f}(\mathbf{x})$ is a Lipschitz continuous vector field on E , such that the quantity $\nabla \mathbf{f}(\mathbf{x}) := \frac{\partial f_1}{\partial x_1}(\mathbf{x}) + \frac{\partial f_2}{\partial x_2}(\mathbf{x})$ is not zero almost everywhere over any subregion of E and is of the same sign almost everywhere in E . Then E does not contain closed trajectories of $\dot{\mathbf{x}} = \mathbf{f}(\mathbf{x})$, where $\mathbf{x} = \begin{pmatrix} x_1 \\ x_2 \end{pmatrix}$ and $\mathbf{f} = \begin{pmatrix} f_1 \\ f_2 \end{pmatrix}$.

3. STABILITY OF AN EQUILIBRIUM AT THE BIFURCATION POINT

For $\mu = 0$, the dynamics of the system (1) is described by the continuous, conewise linear system

$$\dot{\mathbf{x}} = \mathbf{f}(\mathbf{x}) = A_i \mathbf{x}, \quad \mathbf{x} \in \mathcal{S}_i. \quad (2)$$

To analyse the dynamics of the conewise affine system, the stability of the equilibrium of a conewise linear system

is important. Therefore, in this section, we will recall the stability result of Arapostathis and Broucke (2007). For the sake of brevity, in this paper, we restrict ourselves to the case of continuous systems.

If (2) contains one or more visible eigenvectors, then the stability of the origin is determined by the eigenvalues corresponding to these eigenvectors. In conewise linear systems (2) without visible eigenvectors, trajectories exhibit a spiralling motion around the origin, visiting each region \mathcal{S}_i , $i = 1, \dots, m$, once per rotation. Stability results are obtained for the spiralling motion by computation of a return map.

In the absence of visible eigenvectors, a trajectory in the region \mathcal{S}_i , $i = 1, \dots, m$, will traverse this region in finite time. The position \mathbf{x}_0 where a trajectory enters this region at time $t_0 = 0$ is located on the boundary $\Sigma_{i-1,i}$, such that \mathbf{x}_0 can be expressed as $\mathbf{x}_0 = p^i \mathbf{t}_{i-1,i}$. Furthermore, this trajectory will cross $\Sigma_{i,i+1}$ at a finite time t_i . The position of this crossing can be given as: $\mathbf{x}(t_i) = p^{i+1} \mathbf{t}_{i,i+1}$. Since the dynamics inside the cone are linear, the time t_i can be solved for, such that $\mathbf{x}(t_i)$ is parallel to $\mathbf{t}_{i,i+1}$. In this manner, in Arapostathis and Broucke (2007), expressions for the traversal time and crossing positions are derived. The crossing positions are linear in p^i . Using such analysis, we can derive expressions for a scalar M_i , such that $p^{i+1} = M_i p^i$.

First, the position vectors \mathbf{x} and tangency vectors \mathbf{t} are represented in a new coordinate frame:

$$\bar{\mathbf{x}} = P_i^{-1} \mathbf{x}, \quad \text{for } \bar{\mathbf{x}} \in \bar{\mathcal{S}}_i := \{\bar{\mathbf{x}} \in \mathbb{R}^2 | \bar{\mathbf{x}} = P_i^{-1} \mathbf{x}, \mathbf{x} \in \bar{\mathcal{S}}_i\}, \quad (3)$$

where P_i is given by the real Jordan decomposition of A_i , yielding $A_i = P_i J_i P_i^{-1}$. This decomposition distinguishes three cases.

Case 1: If A_i has complex eigenvalues, then $J_i = \begin{bmatrix} a_i & -\omega_i \\ \omega_i & a_i \end{bmatrix}$, where a_i and ω_i are real constants and $\omega_i > 0$. Define $\Theta(\mathbf{a}_1, \mathbf{a}_2)$ to be the angle in counter clockwise direction from vector \mathbf{a}_1 to vector \mathbf{a}_2 . Herewith,

$$M_i = \frac{\|\tilde{\mathbf{t}}_{i-1,i}\|}{\|\tilde{\mathbf{t}}_{i,i+1}\|} e^{\frac{a_i}{\omega_i} \Theta(\tilde{\mathbf{t}}_{i-1,i}, \tilde{\mathbf{t}}_{i,i+1})}, \quad (4)$$

where $\mathbf{e}_1 := (1 \ 0)^T$ and $\mathbf{e}_2 := (0 \ 1)^T$.

Case 2: If A_i has two distinct real eigenvalues λ_{ai} and λ_{bi} and two distinct eigenvectors, then $J_i = \begin{bmatrix} \lambda_{ai} & 0 \\ 0 & \lambda_{bi} \end{bmatrix}$ and

$$M_i = \left| \frac{\mathbf{e}_2^T \tilde{\mathbf{t}}_{i,i+1}}{\mathbf{e}_2^T \tilde{\mathbf{t}}_{i-1,i}} \right|^{\frac{\lambda_{ai}}{\lambda_{bi} - \lambda_{ai}}} \left| \frac{\mathbf{e}_1^T \tilde{\mathbf{t}}_{i,i+1}}{\mathbf{e}_1^T \tilde{\mathbf{t}}_{i-1,i}} \right|^{\frac{\lambda_{bi}}{\lambda_{ai} - \lambda_{bi}}}. \quad (5)$$

Case 3: If A_i has two equal real eigenvalues λ_i with geometric multiplicity 1, then $J_i = \begin{bmatrix} \lambda_i & 1 \\ 0 & \lambda_i \end{bmatrix}$ and

$$M_i = \left| \frac{\mathbf{e}_2^T \tilde{\mathbf{t}}_{i-1,i}}{\mathbf{e}_2^T \tilde{\mathbf{t}}_{i,i+1}} \right| e^{\lambda_i \left(\frac{\mathbf{e}_1^T \tilde{\mathbf{t}}_{i,i+1}}{\mathbf{e}_2^T \tilde{\mathbf{t}}_{i,i+1}} - \frac{\mathbf{e}_1^T \tilde{\mathbf{t}}_{i-1,i}}{\mathbf{e}_2^T \tilde{\mathbf{t}}_{i-1,i}} \right)}. \quad (6)$$

By computation of the scalars M_i with (4),(5) or (6) for each cone \mathcal{S}_i , $i = 1, \dots, m$, one can compute the return map between the positions \mathbf{x}_k and \mathbf{x}_{k+1} of two subsequent crossings of the trajectory $\mathbf{x}(t)$ with the boundary Σ_{m1} :

$$\mathbf{x}_{k+1} = \Lambda \mathbf{x}_k, \quad (7)$$

where

$$\Lambda = \frac{p^{m+1}}{p^1} = \prod_{i=1}^m M_i. \quad (8)$$

Now, we can derive the stability of system (2).

Theorem 3. (Arapostathis and Broucke (2007)). The origin of the continuous, conewise linear system (2) is globally asymptotically stable if and only if

- (i) All visible eigenvectors are associated with eigenvalues $\lambda < 0$,
- (ii) if no visible eigenvectors exist, then it should hold that $\Lambda < 1$, with Λ defined in (8), (4), (5) and (6).

4. BIFURCATION ANALYSIS

The limit sets that can occur in planar continuous systems are equilibria, closed orbits and homoclinic or heteroclinic orbits. To analyse the occurring bifurcations, we are interested in characterisation of these limit sets, including their local stability, for different values of the system parameter μ . In this section, we adopt the following assumption.

Assumption 1. All matrices A_i , $i = 1, \dots, m$, of (1) are invertible.

Note, that this assumption implies that only distinct points \mathbf{x}_{eq} can exist in the continuous system (1) that satisfy $\mathbf{f}(\mathbf{x}_{eq}, \mu) = \mathbf{0}$. Solutions of conewise affine systems as given in (1) scale linearly with the bifurcation parameter μ , as formalised in the following lemma.

Lemma 4. Consider two continuous conewise affine systems $\dot{\mathbf{x}} = \mathbf{f}(\mathbf{x}) + \mu_i \mathbf{b}$, $\mu_i \in (0, \infty)$, $i = 1, 2$, where $\mathbf{f}(\cdot)$ is piecewise linear with cone-shaped regions. If $\phi_1(t)$ is a solution of $\dot{\mathbf{x}} = \mathbf{f}(\mathbf{x}) + \mu_1 \mathbf{b}$, then $\phi_2(t) = \frac{\mu_2}{\mu_1} \phi_1(t)$ is a solution of $\dot{\mathbf{x}} = \mathbf{f}(\mathbf{x}) + \mu_2 \mathbf{b}$.

From this lemma, we conclude that a complete bifurcation diagram can be obtained by finding all existing limit sets at an arbitrary negative, and an arbitrary positive parameter μ , and at the bifurcation point with $\mu = 0$. Subsequently, with Lemma 4, the limit sets for all parameters μ can be found. The conewise affine system (1) is conewise linear if $\mu = 0$. The dynamical behaviour of (1) at $\mu = 0$ has been analysed in the previous section.

In continuous, conewise affine systems with $\mu \neq 0$, the trajectories will be tangent to a specific boundary Σ_{ij} at zero, one, or all points on this boundary. We suppose trajectories are tangent to the boundary at one or no points on each boundary. These points will be called *tangent points*. We will determine all tangent points of the conewise affine system and compute trajectories in forward and backward time through these tangent points and through the origin. In addition, when a node or saddle point exists, the stable and unstable manifold of this point are computed. Computation of this finite number of trajectories yields insight in the possible behaviour of all trajectories. With these manifolds and trajectories, for each domain \mathcal{S}_i , we can identify which subsets of \mathcal{S}_i contain trajectories that leave or enter this domain and through which boundary. Therewith, one can identify what sequence of boundaries and cones can possibly be visited by closed orbits.

For each of these sequences, a return map can be derived. Hence, finding fixed points in these maps is equivalent to finding closed orbits of (1). However, the domain of these maps may be unbounded, such that no feasible computational approach would exist to find all fixed points in the map. Below, we will present two theorems, that can be used to find a halfline in state space, that cannot be traversed by any closed orbit. Existence of

such a halfline will reduce the domain of the map, in which fixed points may exist, to a bounded domain.

Theorem 5. Consider the continuous, conewise affine system (1) with constant $\mu \neq 0$. Suppose the system does not contain visible eigenvectors.

Construct a system

$$\dot{\mathbf{y}} = \mathbf{f}(\mathbf{y}) = A_i \mathbf{y}, \mathbf{y} \in \mathcal{S}_i. \quad (9)$$

by setting $\mu = 0$ in (1). Let Λ for this system be defined in (8), (4), (5) and (6).

When $\Lambda \neq 1$, there exists an $\mathbf{x}_F \in \Sigma_{m1} \setminus \{\mathbf{0}\}$, such that all points in the halfline $R := \{\mathbf{x} \in \Sigma_{m1} \mid \|\mathbf{x}\| \geq \|\mathbf{x}_F\|\}$ are not part of a closed orbit of (1).

A similar result will be formulated for systems with visible eigenvectors.

Theorem 6. Consider system (1), satisfying Assumption 1. If visible eigenvectors exist and all boundaries Σ_{ij} do not contain a visible eigenvector of A_i or A_j , then there exists a halfline $H \subset \mathbb{R}^2$, such that closed orbits can not contain a point $\mathbf{x}_0 \in H$.

When analysing systems described by (1), Theorems 1, 2, 5 and 6 can be exploited to exclude closed orbits in specific regions of state space. However, in certain cases, existence of closed orbits can not be excluded in some parts of the domain \mathbb{R}^2 .

To find all closed orbits, return maps are constructed for all possible sequences of cones and boundaries. A logical choice for the Poincaré section, on which the return maps are defined, are the positions where trajectories cross a certain boundary. This is possible for all closed orbits that traverse multiple cones. Closed orbits inside a single cone encircle a center, since the dynamics in that cone are affine. In the following section, partial maps will be constructed. A partial map describes the position of a trajectory before and after the visit of a specific cone \mathcal{S}_i , $i = 1, \dots, m$. Subsequently, we discuss how to combine these partial maps to obtain the return map.

Trajectories visiting a cone \mathcal{S}_i

In the derivation of Theorem 3, a trajectory of a conewise linear system is followed inside a specific cone \mathcal{S}_i during the traversal of this cone. Since the trajectory during this traversal is described by the linear differential equation $\dot{\mathbf{x}} = A_i \mathbf{x}$, an analytical expression for the trajectory $\mathbf{x}(t)$ with initial position $\mathbf{x}_0 \in \Sigma_{i-1,i}$ can be derived. With this expression, the traversal time t_i and final position $\mathbf{x}(t_i)$ are obtained. Here, a similar approach will be used for the conewise affine system (1).

For a given cone \mathcal{S}_i , $i = 1, \dots, m$, and given boundaries, where the trajectory enters or leaves this domain, the partial map will be constructed that gives the exit position as a function of the position, where \mathcal{S}_i is entered. Since (1) is autonomous, we can assume the domain \mathcal{S}_i is entered at the time $t = 0$. We study a trajectory traversing \mathcal{S}_i from the boundary Σ_- towards the boundary Σ_+ in a finite time t_i . Therefore, the trajectory $\mathbf{x}(t)$ satisfies $\mathbf{x}(t) \in \mathcal{S}_i$, $t \in (0, t_i)$, $\mathbf{x}(0) \in \Sigma_-$ and $\mathbf{x}(t_i) \in \Sigma_+$. We define the maps $\mathbf{g}_i : D_i \subset \Sigma_- \rightarrow I_i \subset \Sigma_+$, describing the position $\mathbf{x}(t_i)$ as a function of $\mathbf{x}(0)$. Expressions for \mathbf{g}_i are derived in Appendix A.

Construction of the return map

The stable or unstable manifolds of nodes and saddle points and the trajectories through tangent points and the origin are computed. Therewith, for each domain \mathcal{S}_i , we can identify what subsets of \mathcal{S}_i contain trajectories that

leave or enter this domain and through which boundary. Combining these domains, one can identify what sequences of boundaries and cones can contain closed orbits. A return map is computed for each sequence to find all closed orbits.

For example, suppose we want to study whether there exist one or more closed orbits that traverse the regions and boundaries $\mathcal{S}_1, \Sigma_{12}, \mathcal{S}_2, \Sigma_{23}, \mathcal{S}_3, \Sigma_{31}$ in this order. A Poincaré section is taken at the moments where trajectories cross Σ_{31} , the corresponding return map is denoted as $M : D_M \subset \Sigma_{31} \rightarrow I_M \subset \Sigma_{31}$. Therewith, $M(\mathbf{x}_k)$ describes the first crossing of a trajectory $\mathbf{x}(t)$, $t > 0$ with boundary Σ_{31} , where $\mathbf{x}(t)$ corresponds to the initial condition $\mathbf{x}(0) = \mathbf{x}_k \in D_M$. Define $\mathbf{g}_1 : D_1 \subset \Sigma_{m1} \rightarrow I_1 \subset \Sigma_{12}$ according to (A.7), (A.9) or (A.11), where $\Sigma_- = \Sigma_{m1}$ and $\Sigma_+ = \Sigma_{12}$. In addition, define $\mathbf{g}_2 : D_2 \subset \Sigma_{12} \rightarrow I_2 \subset \Sigma_{23}$ and $\mathbf{g}_3 : D_3 \subset \Sigma_{23} \rightarrow I_3 \subset \Sigma_{m1}$ in a similar fashion. From a combination of \mathbf{g}_1 , \mathbf{g}_2 and \mathbf{g}_3 , one obtains the return map $M(\mathbf{x}_k) = \mathbf{g}_3 \circ \mathbf{g}_2 \circ \mathbf{g}_1(\mathbf{x}_k)$.

Since M is a return map, every fixed point of this map is on a closed orbit. Furthermore, each closed orbit of (1), that traverses the boundaries and regions in the sequence $\mathcal{S}_1, \Sigma_{12}, \mathcal{S}_2, \Sigma_{23}, \mathcal{S}_3, \Sigma_{31}$, yields a fixed point in M .

The return map M can be computed for the possible sequences of cones and boundaries. By determining the fixed points of such maps, the existence or absence of closed orbits can be investigated. Each return map is continuous, since (1) is Lipschitz continuous, and trajectories of this class of systems are continuous with respect to initial conditions, see Khalil (2002), Theorem 3.4. Furthermore, the Euclidean norm of the map, $\|M(\mathbf{x})\|$, is monotonously increasing in $\|\mathbf{x}\|$. Monotonicity follows from the fact that the time-reversed system of (1) is Lipschitz as well, such that the inverse of M should exist and should be unique. The norm $\|M(\mathbf{x})\|$ has to be increasing in $\|\mathbf{x}\|$. Otherwise, there exist points $\mathbf{x}_a, \mathbf{x}_b \in D_M$, where $\|\mathbf{x}_a\| < \|\mathbf{x}_b\|$ and $\|M(\mathbf{x}_a)\| > \|M(\mathbf{x}_b)\|$. In that case the trajectories from \mathbf{x}_a and \mathbf{x}_b have to cross each other before they return to the Poincaré section. This is not possible in planar autonomous systems. The fact that the return map is continuous and monotonously increasing can be used in the computational approach to find all fixed points.

Procedure to obtain all limit sets

In this section, a stepwise procedure is developed, such that all limit sets of (1) are found for negative, positive and zero bifurcation parameter μ . With this procedure, the bifurcations of the continuous, conewise affine system (1) can be described entirely.

Lemma 4 implies, that only an arbitrary positive and negative μ , and $\mu = 0$, should be studied to obtain the full bifurcation diagram. Theorems 1 and 2 are used to exclude the existence of closed orbits. For systems without visible eigenvectors, Theorem 5 supplies a bound to exclude closed orbits far away from the origin. If visible eigenvectors exist, Theorem 6 can be applied to bound the domain, in which closed orbits can occur. When Theorem 5 or 6 can be applied, a bounded domain for the return map remains, such that it is computationally feasible to find all fixed points of the return map with a numerical method. When certain sequences of boundaries and cones may contain closed orbits, return maps will be constructed.

The following procedure yields a bifurcation diagram of (1) that contains all limit sets.

1. Identify all equilibria for positive and negative μ , i.e. the points $\mathbf{x} \in \mathbb{R}^2$ where $\mathbf{f}(\mathbf{x}) = \mathbf{0}$, with $\mathbf{f}(\mathbf{x})$ given in (1).

2. Study the stability of the equilibrium point $\mathbf{x} = \mathbf{0}$ at $\mu = 0$ using Theorem 3. Identify all visible eigenvectors of A_i , $i = 1, \dots, m$.

3. For both an arbitrary fixed $\mu < 0$ and $\mu > 0$:

- a. Compute points where the vector field is tangent to the boundaries. Subsequently, compute trajectories through these tangent points and through the origin for a finite time. In addition, compute the eigenvalues of the matrices A_i , $i = 1, \dots, m$, when an equilibrium exists inside the corresponding cone \mathcal{S}_i . When an equilibrium with real eigenvalues exists, compute the stable and unstable manifolds by simulating a trajectory emanating from or converging to this equilibrium in the direction of the eigenvectors. To check whether homoclinic or heteroclinic orbits exist, investigate whether stable and unstable manifolds coincide.

- b. Identify, if possible, certain domains that cannot contain closed orbits. First, identify the value of $\text{tr}(A_i)$, $i = 1, \dots, m$ for each region \mathcal{S}_i , i.e. the trace of the matrices A_i . According to Theorem 2, a closed orbit should visit regions \mathcal{S}_i where the traces $\text{tr}(A_i)$ have opposite sign or are zero, since $\nabla \mathbf{f}(\mathbf{x}) = \text{tr}(A_i)$ for $\mathbf{x} \in \mathcal{S}_i$. Second, apply Theorem 1. For example, no closed orbits are possible that encircle one hyperbolic saddle and one focus, since the sum of indices of these points equals zero. Third, determine which equilibria should be encircled by possibly existing closed orbits in order to satisfy Theorem 1. Finally, when an unbounded domain remains that may contain closed orbits, identify halflines R or H as defined in Theorem 5 or Theorem 6. Investigate what sequences of cones and boundaries can still be traversed by closed orbits. For these sequences of cones and boundaries, a return map will be constructed.

- c. Compute the maps \mathbf{g}_i for the cones \mathcal{S}_i that may be traversed by a closed orbit. These maps are given in (A.7), (A.9) and (A.11). Combination of these maps yields the return maps for the possible sequences of cones and boundaries. Note, that when a halfline R or H , as defined in Theorem 5 or 6, respectively, is found that can not be crossed by a closed orbit, the domain of these maps, where fixed points may exist, will be bounded. Determine the fixed points of all possible return maps in a numerical manner. Compute the local derivative of the return map at this fixed point, since this determines the stability of the closed orbit.

4. Identify what limit sets appear, disappear or change their local stability for changing μ . Application of Lemma 4 with respect to the limit sets for a given $\mu < 0$ or $\mu > 0$ yields all limit sets for $\mu \neq 0$. Combination with the piecewise linear stability result gives a bifurcation diagram, containing all changes in limit sets and their stability.

The procedure given above yields all changes in the limit sets of the system. The procedure finds all closed orbits, since for each conewise affine system (1), a finite number of return maps can be determined, that may contain fixed points. Computation of each of these return maps yields all closed orbits.

5. ILLUSTRATIVE EXAMPLE

Consider the continuous system:

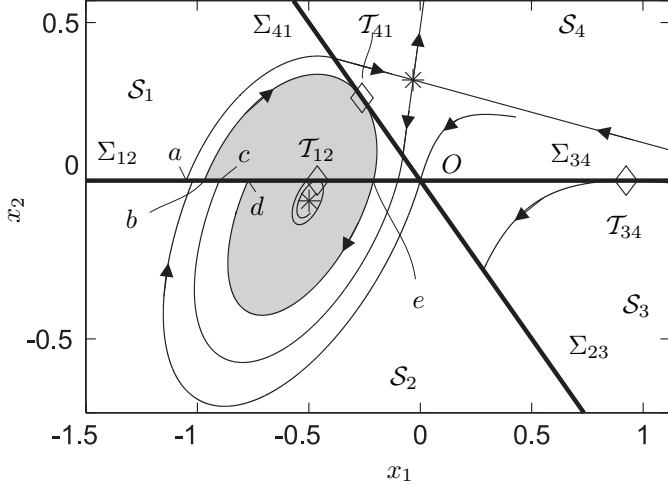


Fig. 1. Phase portrait of system (10) for $\mu = 0.5$ with trajectories through tangent points and the origin. In addition, the equilibria are depicted with asterisks, and the manifolds of the saddle point are shown.

$$\dot{\mathbf{x}} = \begin{cases} A_1 \mathbf{x} + \mu \mathbf{b}, & x \in \mathcal{S}_1 := \{\mathbf{x} \in \mathbb{R}^2 \mid \mathbf{n}_{41}^T \mathbf{x} < 0 \wedge \mathbf{n}_{12}^T \mathbf{x} > 0\}, \\ A_2 \mathbf{x} + \mu \mathbf{b}, & x \in \mathcal{S}_2 := \{\mathbf{x} \in \mathbb{R}^2 \mid \mathbf{n}_{12}^T \mathbf{x} < 0 \wedge \mathbf{n}_{23}^T \mathbf{x} > 0\}, \\ A_3 \mathbf{x} + \mu \mathbf{b}, & x \in \mathcal{S}_3 := \{\mathbf{x} \in \mathbb{R}^2 \mid \mathbf{n}_{23}^T \mathbf{x} < 0 \wedge \mathbf{n}_{34}^T \mathbf{x} > 0\}, \\ A_4 \mathbf{x} + \mu \mathbf{b}, & x \in \mathcal{S}_4 := \{\mathbf{x} \in \mathbb{R}^2 \mid \mathbf{n}_{34}^T \mathbf{x} < 0 \wedge \mathbf{n}_{41}^T \mathbf{x} > 0\}, \end{cases} \quad (10)$$

where the normal vectors are chosen as $\mathbf{n}_{12} = [0 \ 1]^T$, $\mathbf{n}_{23} = \frac{1}{\sqrt{2}}[-1 \ -1]^T$, $\mathbf{n}_{34} = [0 \ -1]^T$, $\mathbf{n}_{41} = \frac{1}{\sqrt{2}}[1 \ 1]^T$. The vector $\mathbf{b} = [\cos(0.375\pi) \ \sin(0.375\pi)]^T$ and $\mu \in \mathbb{R}$ is the bifurcation parameter. The phase portrait of this system for $\mu = -0.5$ is shown in Figure 1. The matrices A_i are $A_1 = \begin{bmatrix} -0.5 & 1 \\ -1 & 0 \end{bmatrix}$, $A_2 = \begin{bmatrix} -0.5 & 0.91 \\ -1 & 0.58 \end{bmatrix}$, $A_3 = \begin{bmatrix} -1 & 0.41 \\ 0.5 & 2.08 \end{bmatrix}$, $A_4 = \begin{bmatrix} -1 & 0.5 \\ 0.5 & 1.5 \end{bmatrix}$. System (10) will be analysed with the given procedure:

1. For $\mu < 0$, two equilibria exist, with positions $\mathbf{x} = -\mu A_2^{-1} \mathbf{b}$ in \mathcal{S}_2 and $\mathbf{x} = -\mu A_4^{-1} \mathbf{b}$ in \mathcal{S}_4 . For $\mu > 0$, no equilibria exist.
2. At $\mu = 0$, the conewise linear dynamics is unstable, since the visible eigenvector in \mathcal{S}_4 corresponds to an unstable eigenvalue. In addition, one visible eigenvector in \mathcal{S}_3 exists, that corresponds to a stable eigenvalue.
3. For $\mu = -0.5$:
 - a. On Σ_{12} , Σ_{34} and Σ_{41} , there exist points where the vector field is tangent to the boundary, i.e. points \mathcal{T}_{12} , \mathcal{T}_{34} and \mathcal{T}_{41} , respectively. Trajectories through these points and the origin are shown in Figure 1. An unstable focus exist in \mathcal{S}_2 , since the eigenvalues of A_2 are $0.42 \pm 0.79i$, where $i^2 = -1$. A saddle point exist in \mathcal{S}_4 with eigenvalues -1.10 and 1.60 . The depicted stable and unstable manifolds of this point are shown and do not form a homoclinic orbit.
 - b. The trace $\text{tr}(A_1) < 0$, whereas all other traces $\text{tr}(A_i) > 0$, $i = 2, 3, 4$. Therefore, application of Theorem 2 yields that each possible closed orbit visits \mathcal{S}_1 . To satisfy Theorem 1, closed orbit(s) should encircle the focus without encircling the saddle point.

By studying the depicted trajectories, one can conclude, that no closed orbit can traverse $\Sigma_{12} \setminus [O, a]$, since these trajectories cannot encircle the

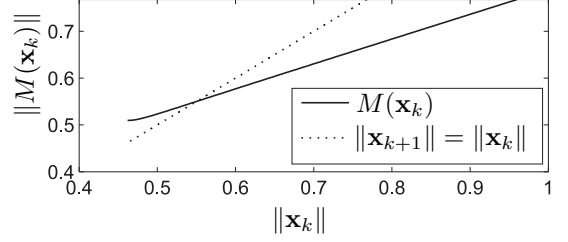


Fig. 2. Combined map M of (10) with $\mu = -0.5$.

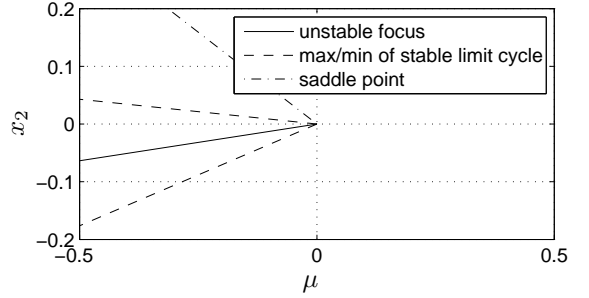


Fig. 3. Bifurcation diagram of (10) with the bifurcation parameter μ .

focus without encircling the saddle point, which is required according to Theorem 1. Furthermore, closed orbits can not traverse the interior of the line $[a, b]$, since trajectories through this open line will arrive at the line $[c, d]$ in finite time, and enter the positively invariant region that is depicted gray in Figure 1. Now, one can conclude, that possible closed orbits visit only the regions \mathcal{S}_1 and \mathcal{S}_2 , such that they should be contained in the domain, that is depicted gray. This implies, that all closed orbits traverse the line $[\mathcal{T}_{12}, e]$.

- c. Existing closed orbits should traverse the line $[\mathcal{T}_{12}, e]$. We construct a map $\mathbf{g}_2 : [\mathcal{T}_{12}, e] \rightarrow [d, \mathcal{T}_{12}]$, that yields the position $\mathbf{g}_2(\mathbf{x})$ where a trajectory leaves the cone \mathcal{S}_2 when this cone was entered at \mathbf{x} . Similarly, the map $\mathbf{g}_1 : [b, \mathcal{T}_{12}] \rightarrow [\mathcal{T}_{12}, e]$ is computed. The maps are computed according to (A.6) and (A.7). The return map $M := \mathbf{g}_1 \circ \mathbf{g}_2(\mathbf{x})$ contains one fixed point, as shown in Figure 2. One stable limit cycle exists that contains $\mathbf{x} = (-0.55 \ 0)^T$.

For $\mu = 0.5$ no equilibrium point of (10) exists, such that according to Theorem 1, no closed orbits can exist.

4. With the analysis above and application of Lemma 4, the bifurcation diagram is constructed, as given in Figure 3. Both the limit cycle, focus and saddle exist only for $\mu < 0$. For $\mu = 0$, unstable behaviour is observed. This bifurcation can not occur in smooth dynamical systems.

6. CONCLUSIONS

A procedure is presented that yields a complete analysis of bifurcating equilibria in continuous, conewise affine systems. Existence of equilibria, homoclinic and heteroclinic orbits are found in a trivial manner. To find all possible closed orbits, the theoretical results are combined with a study of the derived return maps.

The procedure is useful to assess the parameter dependency of equilibria of a system, when the dynamics of this system is conewise affine. Furthermore, the dynamics in the neighbourhood of an equilibrium of any piecewise

smooth system can be approximated as a conewise affine system. In this manner, the local bifurcations of equilibria in all planar, continuous, piecewise smooth systems can be investigated with the presented procedure.

The results of this work can be extended to a more general class of discontinuous, conewise affine systems, that are Filippov systems. With this extension, mechanical systems with Coulomb friction could be analysed.

REFERENCES

- Arapostathis, A. and Broucke, M.E. (2007). Stability and controllability of planar, conewise linear systems. *Syst. & Control Lett.*, 56(2), 150–158.
- di Bernardo, M., Budd, C.J., Champneys, A.R., and Kowalczyk, P. (2008a). *Piecewise-smooth dynamical systems*, volume 163 of *Applied Mathematical Sciences*. Springer verlag, London.
- di Bernardo, M., Budd, C.J., Champneys, A.R., Kowalczyk, P., Nordmark, A.B., Tost, G.O., and Piironen, P.T. (2008b). Bifurcations in nonsmooth dynamical systems. *SIAM Rev.*, 50(4), 629–701.
- Biamond, J.J.B., van de Wouw, N., and Nijmeijer, H. (2009). Nonsmooth bifurcations of equilibria in planar continuous systems. *submitted to Nonlinear Anal. Hybrid Syst.*
- Branicky, M.S. (1998). Multiple Lyapunov functions and other analysis tools for switched and hybrid systems. *IEEE Trans. Autom. Control*, 43, 475–482.
- Camlibel, M.K., Heemels, W.P.M.H., and Schumacher, J.M. (2008). Algebraic necessary and sufficient conditions for the controllability of conewise linear systems. *IEEE Trans. Autom. Control*, 53, 762–774.
- Coddington, E.A. and Levinson, N. (1955). *Theory of Ordinary differential equations*. International Series in Pure and Applied Mathematics. McGraw-Hill, New York.
- Coombes, S. (2008). Neuronal networks with gap junctions: a study of piecewise linear planar neuron models. *SIAM J. Appl. Dyn. Syst.*, 7(3), 1101–1129.
- Hartman, P. (1964). *Ordinary differential equations*. John Wiley & Sons, New York.
- Khalil, H.K. (2002). *Nonlinear Systems*. Prentice Hall, Upper Saddle River, third edition.
- Leine, R.I. (2006). Bifurcations of equilibria in non-smooth continuous systems. *Physica D*, 223(1), 121–137.
- Leine, R.I., van Campen, D.H., and van de Vrande, B.L. (2000). Bifurcations in nonlinear discontinuous systems. *Nonl. Dyn.*, 23, 105–164.
- Leine, R.I. and Nijmeijer, H. (2004). *Dynamics and bifurcation of non-smooth mechanical systems*, volume 18 of *Lecture notes on applied and computational mechanics*. Springer verlag, Berlin.
- Liberzon, D. (2003). *Switching in Systems and Control*. Systems and Control: Foundations & Applications. Birkhäuser, Boston.
- Nordmark, A.B. (1991). Non-periodic motion caused by grazing incidence in an impact oscillator. *J. Sound Vib.*, 145(2), 279–297.
- Oberle, H.J. and Rosendahl, R. (2006). Numerical computation of a singular-state subarc in an economic optimal control model. *Optim. Control Appl. Methods*, 27(4), 211–235.

Appendix A. COMPUTATION OF PARTIAL MAPS

We study a trajectory traversing \mathcal{S}_i from the boundary Σ_- towards the boundary Σ_+ in a finite time t_i . To analyse

this trajectory in the cone \mathcal{S}_i , a new coordinate frame is introduced:

$$\tilde{\mathbf{x}} = P_i^{-1} \mathbf{x} + \mu P_i^{-1} A_i^{-1} \mathbf{b}, \quad \mathbf{x} = P_i \tilde{\mathbf{x}} - \mu A_i^{-1} \mathbf{b}, \quad (\text{A.1})$$

where P_i is given by the real Jordan decomposition, such that $A_i = P_i J_i P_i^{-1}$. The dynamics of (1) in this cone become:

$$\dot{\tilde{\mathbf{x}}} = J_i \tilde{\mathbf{x}}, \quad \text{for } t \in [0, t_i]. \quad (\text{A.2})$$

The initial condition $\mathbf{x}_0 = p^i \mathbf{t}_- \in \Sigma_-$ yields $\tilde{\mathbf{x}}_0 = p^i \tilde{\mathbf{t}}_- + \mu P_i^{-1} A_i^{-1} \mathbf{b}$, where $\tilde{\mathbf{t}}_- := P_i^{-1} \mathbf{t}_-$.

There exists a crossing of the trajectory with the boundary Σ_+ at time t_i . Suppose this crossing occurs at $\mathbf{x}(t_i) = p^{i+1} \mathbf{t}_+$, which is equivalent to $\tilde{\mathbf{x}}(t_i) = p^{i+1} \tilde{\mathbf{t}}_+ + \mu P_i^{-1} A_i^{-1} \mathbf{b}$, where a vector $\tilde{\mathbf{t}}_+ := P_i^{-1} \mathbf{t}_+$ is introduced. Define a normal vector $\tilde{\mathbf{n}}_+ := (\mathbf{e}_1 \mathbf{e}_2^T - \mathbf{e}_2 \mathbf{e}_1^T) \tilde{\mathbf{t}}_+$, yielding:

$$\tilde{\mathbf{n}}_+^T \tilde{\mathbf{x}}(t_i) = \mu \tilde{\mathbf{n}}_+^T P_i^{-1} A_i^{-1} \mathbf{b}. \quad (\text{A.3})$$

Substitution of $\tilde{\mathbf{x}}(t_i) = e^{J_i t_i} \tilde{\mathbf{x}}_0$ in (A.3) yields:

$$\tilde{\mathbf{n}}_+^T e^{J_i t_i} \tilde{\mathbf{x}}_0 = \tilde{\mathbf{n}}_+^T \tilde{\mathbf{x}}_T, \quad (\text{A.4})$$

where we defined the translation vector $\tilde{\mathbf{x}}_T := \mu P_i^{-1} A_i^{-1} \mathbf{b}$.

When the traversal time t_i satisfying (A.4) is found, this time can be used to obtain the traversal position. Integrating (A.2) over a time interval $[0, t_i]$ yields $\tilde{\mathbf{x}}(t_i) = e^{J_i t_i} \tilde{\mathbf{x}}_0$. In the original coordinate frame, this yields:

$$\mathbf{x}(t_i) = P_i e^{J_i t_i} \tilde{\mathbf{x}}_0 - \mu A_i^{-1} \mathbf{b}. \quad (\text{A.5})$$

Substitution of the time t_i satisfying (A.4) in (A.5) forms a map $\mathbf{g}_i : D_i \subset \Sigma_- \rightarrow R_i \subset \Sigma_+$, describing the position of the crossing of $\{\mathbf{x}(t), t > 0, \mathbf{x}(0) \in D_i\}$ with Σ_+ , such that $\mathbf{x}(t_i) = \mathbf{g}_i(\mathbf{x}(0))$. The map \mathbf{g}_i will be computed by distinguishing the three cases.

Case 1: If A_i has complex eigenvalues, then $J_i = \begin{bmatrix} a_i & -\omega_i \\ \omega_i & a_i \end{bmatrix}$, where a_i and ω_i are real and $\omega_i > 0$. Hence, $e^{J_i t} = e^{a_i t} \begin{bmatrix} \cos(\omega_i t) & -\sin(\omega_i t) \\ \sin(\omega_i t) & \cos(\omega_i t) \end{bmatrix}$. Herewith, (A.4) yields:

$$e^{a_i t_i} \cos(\omega_i t_i) \tilde{\mathbf{n}}_+^T \tilde{\mathbf{x}}_0 + e^{a_i t_i} \sin(\omega_i t_i) \tilde{\mathbf{t}}_+^T \tilde{\mathbf{x}}_0 = \tilde{\mathbf{n}}_+^T \tilde{\mathbf{x}}_T. \quad (\text{A.6})$$

This equation can be solved with a numerical solver to obtain the time t_i . This time yields the position:

$$\mathbf{x}(t_i) = -e^{a_i t_i} \sin(\omega_i t_i) P_i (\mathbf{e}_1 \mathbf{e}_2^T - \mathbf{e}_2 \mathbf{e}_1^T) \tilde{\mathbf{x}}_0 + e^{a_i t_i} \cos(\omega_i t_i) P_i \tilde{\mathbf{x}}_0 - \mu A_i^{-1} \mathbf{b}. \quad (\text{A.7})$$

Case 2: If A_i has two real eigenvalues λ_{ai} and λ_{bi} whose eigenvectors are distinct, then $J_i = \begin{bmatrix} \lambda_{ai} & 0 \\ 0 & \lambda_{bi} \end{bmatrix}$. Herewith, (A.4) becomes:

$$e^{\lambda_{ai} t_i} \tilde{\mathbf{n}}_+^T \mathbf{e}_1 \mathbf{e}_1^T \tilde{\mathbf{x}}_0 + e^{\lambda_{bi} t_i} \tilde{\mathbf{n}}_+^T \mathbf{e}_2 \mathbf{e}_2^T \tilde{\mathbf{x}}_0 = \tilde{\mathbf{n}}_+^T \tilde{\mathbf{x}}_T, \quad (\text{A.8})$$

that can be solved with a numerical solver to obtain the smallest time $t_i > 0$. Evaluating (A.5) on this time yields:

$$\mathbf{x}(t_i) = e^{\lambda_{ai} t_i} P_i \mathbf{e}_1 \mathbf{e}_1^T \tilde{\mathbf{x}}_0 + e^{\lambda_{bi} t_i} P_i \mathbf{e}_2 \mathbf{e}_2^T \tilde{\mathbf{x}}_0 - \mu A_i^{-1} \mathbf{b}. \quad (\text{A.9})$$

Case 3: If A_i has two equal real eigenvalues λ_i with geometric multiplicity 1, then $J_i = \begin{bmatrix} \lambda_i & 1 \\ 0 & \lambda_i \end{bmatrix}$. Herewith, (A.4) yields:

$$e^{\lambda_i t_i} \tilde{\mathbf{n}}_+^T \tilde{\mathbf{x}}_0 + t_i e^{\lambda_i t_i} \tilde{\mathbf{n}}_+^T \mathbf{e}_1 \mathbf{e}_2^T \tilde{\mathbf{x}}_0 = \tilde{\mathbf{n}}_+^T \tilde{\mathbf{x}}_T. \quad (\text{A.10})$$

When the smallest $t_i > 0$ satisfying (A.10) is found with a numerical solver, this can be substituted in (A.5), yielding:

$$\mathbf{x}(t_i) = e^{\lambda_i t_i} P_i \tilde{\mathbf{x}}_0 + t_i e^{\lambda_i t_i} P_i \mathbf{e}_1 \mathbf{e}_2^T \tilde{\mathbf{x}}_0 - \mu A_i^{-1} \mathbf{b}. \quad (\text{A.11})$$